CONTROLLED INTERFERENCE COLOR OF THE METAL SURFACE BY COMBINATION OF THE CHEMICAL AND ELECTROCHEMICAL ALUMINUM SURFACE TREATMENT

V. V. Shelkovnikov, G. A. Lyubas, S. V. Korotaev

Novosibirsk institute of organic chemistry N. N. Vorozchtcov SB RAS,
630090, av. Lavrent'eva 9, Novosibirsk, Russia

sciencenano@yandex.ru

The method of the electrochemical and chemical treatment of an aluminum surface to obtain selective coloration of the anodic aluminum oxide films (AAOF) with high index of the reflection and wide range of the color tones was developed. AAOF were formed and both Ag and Au were chemically deposited. The physical and chemical properties of the obtained color AAOF were studied. It was shown that the additional chemical deposition of the noble metal leads to the enhancement of the selective reflection ability and the interference contrast. Silver nanoparticle formation on the surface of the pores after chemical deposition was shown by electron microscopy. The optical reflection spectra at different angles ($10° - 85°$) of metalized AAOF were measured and the effective refractive index ($n \approx 1.6$) and thickness were calculated. The spectral shift of the reflection peaks of nanoporous metalized AAOF was shown to depend on the nature of the marked solvents.

Keywords: selective coloration, nanoporous anodic aluminum oxide films, electrochemical and chemical metallization, nanoparticles.

1. Introduction

When anodized in an acidic electrolyte, aluminum forms a porous oxide with uniform and parallel pores open at top end and sealed at the other. Anodic aluminum oxide film (AAOF) has been the subject of numerous studies due to its porous nature and has numerous practical application. The use of the anodic aluminum oxide on aluminum is an effective way to increase the corrosion stability of the metal. Special interest in this material is raised as a result of its use as a template medium for creating nanostructures inside the pores. Among different approaches to fill materials into the pores of anodic aluminum oxide templates, electrochemical deposition technology has received considerable attention for its simplicity and high efficiency. Different metals including Au, Ag, Cu, and Ni [1–12] and some semiconductors [13] have been deposited into AAOF by electrochemistry. This process is applied for the electrochemical interference coloration of the anodic aluminum to get the protective decorative coating [14]. Little attention has been paid to the possibilities of the double electrochemical and chemical deposition of the two metals on the anodic aluminum oxide surface for coloration. This is quite possible in the case of the chemical reduction of noble metals from their salt solutions on the first electrodeposited active metals such Zn, Bi, Cu, Ni, Co, Fe, Cd, Sn, Pb and others. The conditions and regimes of the aluminum electrochemical anodization and electrochemical and chemical metallization are not investigated from the point of view the influence of the additional

metal deposition on the effect of the interference coloration. Today, we are not aware of any articles on this topic.

The goal of this research is the development of the electrochemical and chemical treatment processes for the aluminum surface to obtain selective coloration of the aluminum anodic films with a high index of reflection and a wide range of color tones.

2.   Experimental Section

Porous anodic oxide films were formed on the metal surface by anodization of Al in acidic solution. Anodization of the samples was processed in 2 % solution of sulfuric acid at 20 °C in potentiostatic mode. The oxidation time, applied voltage magnitude and current density were the following: 1.5 – 50 minutes, 12 – 20 volts and 200 A/m^2, respectively. A high purity (99.95 %) aluminum foil with 0.1 mm thickness was used for fabrication of porous anodic oxide films. The foil was cleaned in a solution of 10 % sodium hydroxide and then electrochemically polished at 60 °C in a mixture of 34 g orthophosphoric acid (specific weight 1.7), 34 g sulfuric acid (specific weight of 1.84), 4 g chromic anhydride, water (to 100 g) at a constant voltage of 12 volts for 2 min to achieve a mirror finished surface. From analysis of the oxidation time and applied voltage magnitude, parameters for the anodic oxidation were optimized. The optimal oxidation time, applied voltage magnitude and current density were the following: 3 – 5 minutes, 12 volts and 200 A/m^2, respectively. Porous alumina was prepared by electrochemical anodization [15] and metallization, into which noble metal nanoparticles were chemically or electrochemically deposited. To improve the interference properties of anodic porous alumina film, three types of processes have been produced: polishing, electrochemical deposition of metal nanoparticles (Cu, Ni) inside the pores of the aluminum oxide and additional chemical deposition of the noble metals (Ag, Au) on the aluminum surface. Electrochemical deposition of nickel particles in pores of anodic alumina was performed using alternating current (potentiostatic regime). The optimal deposition time, applied voltage magnitude, current density and frequency of alternating current were the following: 3 – 4 minutes, 12 - 15 volts, 150 A/m^2 and 50 Hz, respectively. The electrolyte consisted of nickel sulfate (40 kg/m^3), cobalt sulfate (40 kg/m^3) and boric acid (40 kg/m^3). Electrochemical deposition of copper particles in pores of anodic alumina was done using alternating current (potentiostatic mode). The optimal deposition time, applied voltage magnitude, current density and frequency of alternating current were the following: 3 – 4 mins, 12 - 14 volts, 200 - 500 A/m^2 and 50 Hz, respectively. The electrolyte consisted of copper sulfate (50 kg/m^3), magnesium sulfate (20 kg/m^3) and sulfuric acid (to pH = 1). The aim of this procedure, which was to form particles of gold or silver by the exchange reactions layers, went in the following manner. The processing of gold was conducted by a solution of the following composition: chloroauric acid (HAuCl$_4$) (1 kg/m^3), sulfuric acid (to pH = 1 – 2). Silver processing was conducted by a solution of the following composition: silver nitrate (1 kg/m^3), sulfuric acid (to pH = 2). The processing time was 3 – 4 minutes.

Reflection and absorption spectra of the studied films were recorded on a AvaSpec1024 spectrometer. Resolution of spectrometer is about 0.5 nm. The light source was a halogen lamp (AvaLightDHS). The spectra were recorded under various input angles. The range of the input angles of light varied from 10° to 85°, as is shown on the measurement scheme (fig. 1). High-resolution scanning electron microscopy was performed using Zeiss MERLIN VP Compact scanning electron microscope operating at high-resolution mode at 20 kV with 5 nm resolution.
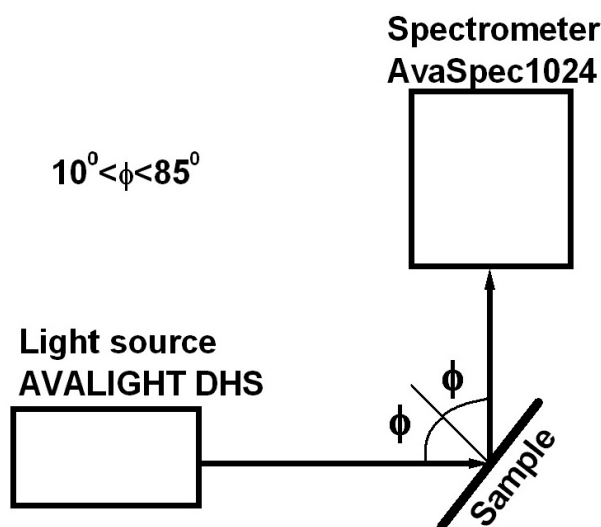
Spectrometer
AvaSpec1024

$10^0 < \phi < 85^0$

Light source
AVALIGHT DHS

ϕ

ϕ

Sample

FIG. 1. Measurement scheme of reflectance spectra

3. Results and Discussion

Immediately after anodization of the poled aluminum and formation of the oxide layer the interference color is not visible. The interference is very weak (curve 4 on the fig. 2) on the thin oxide layer. In our case, the kinetics of the anodic aluminum oxide layer growth is slower than in usual sulfate electrolytes due to the lowered sulfuric acid concentration and the thin layer of anodic aluminum oxide formed. After electrodeposition of the Cu or Ni inside the pores of anodic aluminum oxide the interference color appears, depending on the thickness of the initial oxide layer or on the time of the anodic film growth. Due to the low degree of the metal deposition, the metal absorbance is weak and the interference color is bright. It was shown that the controlled interference color of the metal surface was obtained by combination of the chemical and electrochemical aluminum surface treatment. After additional metal electrodeposition, we observe the growth of the metal nanoparticles absorption and a reduction of the interference color.

The reflection spectra of the aluminum oxide films colored by Cu deposition, in reference to the Al mirror, is shown on the fig. 2. One can observe the growth of the interference minima and maxima of the reflection peaks. The metal cuprum is in the left side in the electrochemical series compared to the silver and gold and it displace the noble metals from the solution of their salts. Both Ag and Au were chemically deposited on the Cu electrodeposited nanoparticles. The additional chemical deposition changes the relationship between interference peaks and leads to a small red shift for the maximum on the left and blue shift for the maximum on the right in the visible spectral range. The chemical deposition of the noble metal on the copper nanoparticles electrodeposited in anodic aluminum oxide leads to a noticeable enhancement of the selective reflectivity of the anodized film (see fig. 2).

The blank AAOF without deposited metals has a very weak, on the noise level interference reflection. The first Cu electrodeposition on anodic aluminum oxide leads to a three-fold amplification of the reflection peaks compared to AAOF. Second chemical deposition of the noble metals leads to the formation of AAOF with Cu–Au nanoparticles. The obtained film showed an additional two-fold amplification of the reflection peaks and enhanced contrast (difference between the maximum and minimum) of the interference peaks.
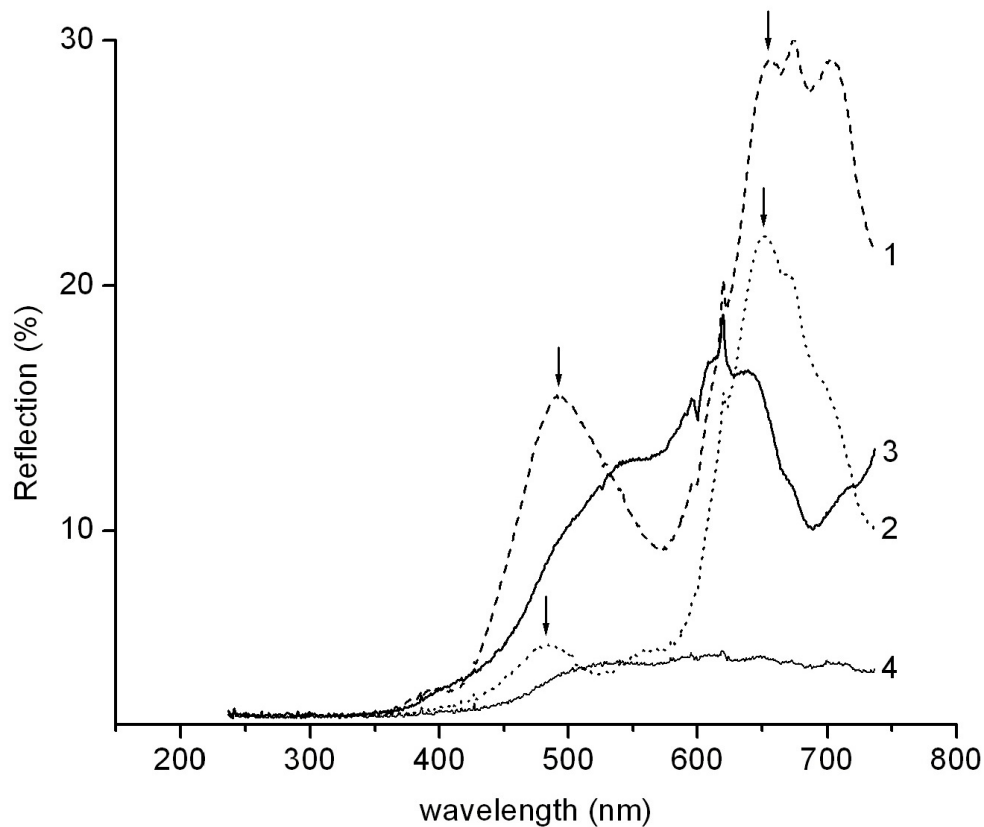
FIG. 2. Reflection spectra of the anodized films with chemical deposited gold (1) and silver (2) nanoparticles by substitution of copper in reference to Al mirror. The solid curve (3) is spectrum of the anodized film with Cu. The solid curve (4) is spectrum of the blank anodized film. It is seen that the difference between the maximum and minimum increases. The input angle of light is 75°

The reflection spectra of the obtained color AAOF were measured under different incident angles of the light and are shown in fig. 3 for AAOF with Cu-Au nanoparticles. One can see that the spectral changes are dependent on the angle, with the interference maxima in the spectra being shifted to the short-wavelength side when the angle of incident light on the sample increases. The appearance of the number of contrasted reflection peaks can be explained by interference phenomena. This is clearly seen in fig. 4, where the reflection spectra of the anodized 20 min films with electrochemical deposited silver nanoparticles are shown. The high contrast interference reflection spectra are shifted one half of phase when changing the input angle from 20° to 40°. The formation of the interference color reflection in anodic aluminum oxide metalized structure is shown schematically in fig. 5.

Both interfaces Al_2O_3/air and Al/Al_2O_3 are partly reflective, and reflectivity is enhanced by the combination of the electrochemical and chemical metal deposition on the anodic aluminum oxide surface. For films with the thickness h, the wavelengths λ of the reflection intensity maxima are given by the interference condition:

$$2h\sqrt{n^2 - \sin^2 \varphi} = m\lambda, \qquad m = 1,\ 2,\ 3,\ \ldots,$$

where n is refractive index, h is film thickness, φ is incident angle corresponding to the maximum with wavelength.
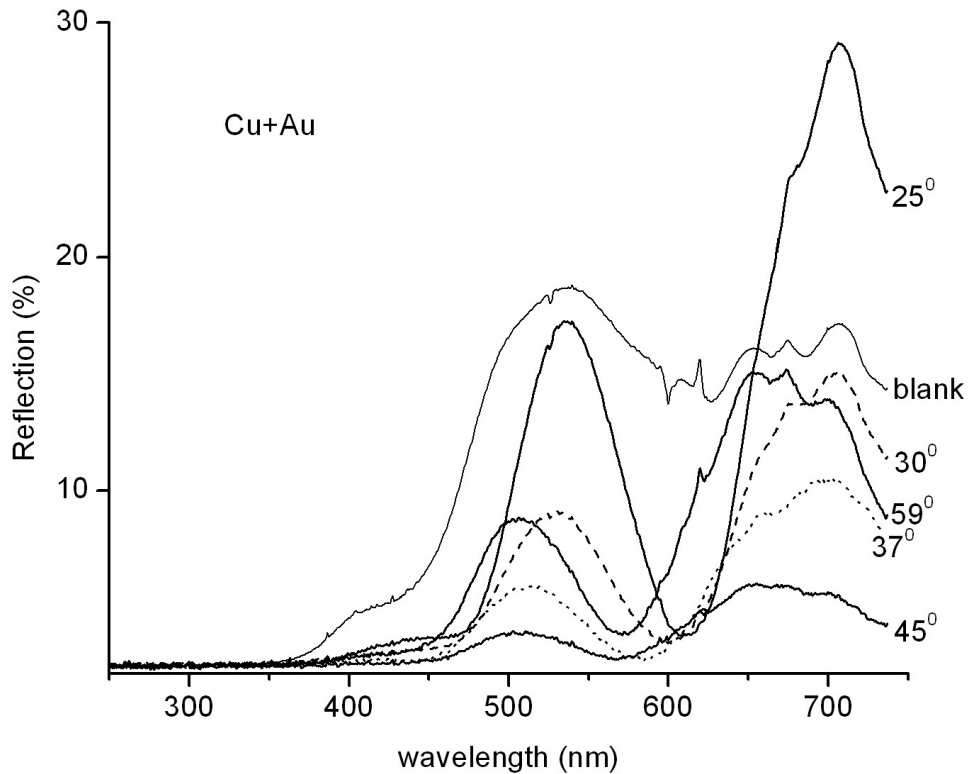
FIG. 3. The reflection spectra under different incident angles. The solid curve (blank) is reflection spectrum of the blank AAOF for the input angle of light 25°

Using the theory of interference in thin films, it is possible to calculate the refractive index (n) and thickness (h) of the film from the angle dependence the reflection peak spectral shift. For the m-th order of the reflection peak, we have next original relationships:

$$h^2 = \frac{m^2\lambda^2}{4(n^2 - \sin^2\varphi)},$$

$$n^2 = \frac{\sin^2\varphi - \dfrac{\lambda_1^2}{\lambda_2^2}\sin^2\theta}{1 - \dfrac{\lambda_1^2}{\lambda_2^2}},$$

where φ is incident angle corresponding to the maximum with wavelength λ_1, θ is incident angle corresponding to the maximum with wavelength λ_2. The angular dispersion of the reflection peak in coordinates ($\lambda^2 \div \sin^2\varphi$) is shown in fig. 6. The experimental points are in good agreement with the modeling theoretical line.

The calculated values for the effective refractive index of the measured films is approximately 1.6. This result is in good agreement with the data obtained by other authors for AAOF [14]. The calculated value of h for the measured film was found to be ~ 0.2 μm.

The obtained metalized AAOF were studied by high-resolution scanning electron microscopy. The electron microscopy image of the film is shown in fig. 7. The Cu–Ag metalized AAOF with high nanopore density and minimal baffle thickness are observed in the image. The diameter of nanopores is about $30 - 50$ nm. The thickness of porous layer is ~ 0.2 μm. This value coincides well with the thickness calculated from the interference reflection angle
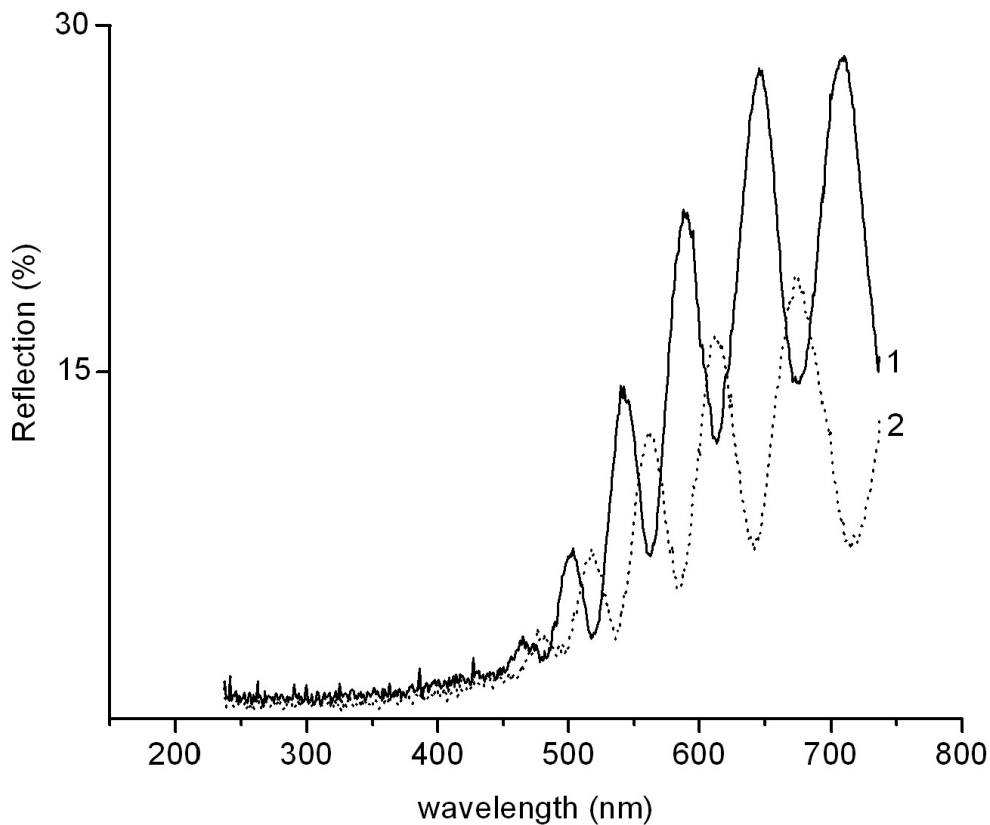
FIG. 4. Reflection spectra of the anodized 20 min films with electrochemical deposited silver nanoparticles in reference to Al mirror. The solid curve (1) is spectrum for the input angle of 20°. The dot curve (2) is spectrum for the input angle of 40°. It is seen that the high contrast interference reflection spectra are shifted one half of phase when changing the input angle from 20° to 40°
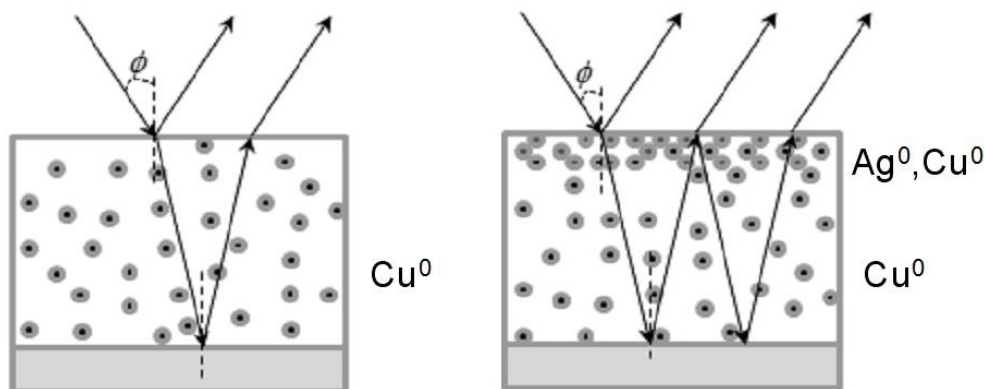
FIG. 5. Scheme of formation of the interference color

dispersion data. The bright spheroid particles on the top of porous film are 20 – 50 nm Ag nanoparticles.

We explain the enhancement of the reflection interference intensity and contrast by the specific deposition of the effective additional metal layer on the anodic aluminum oxide surface leading to the formation of the nanostructure metalized AAOF like the structure of
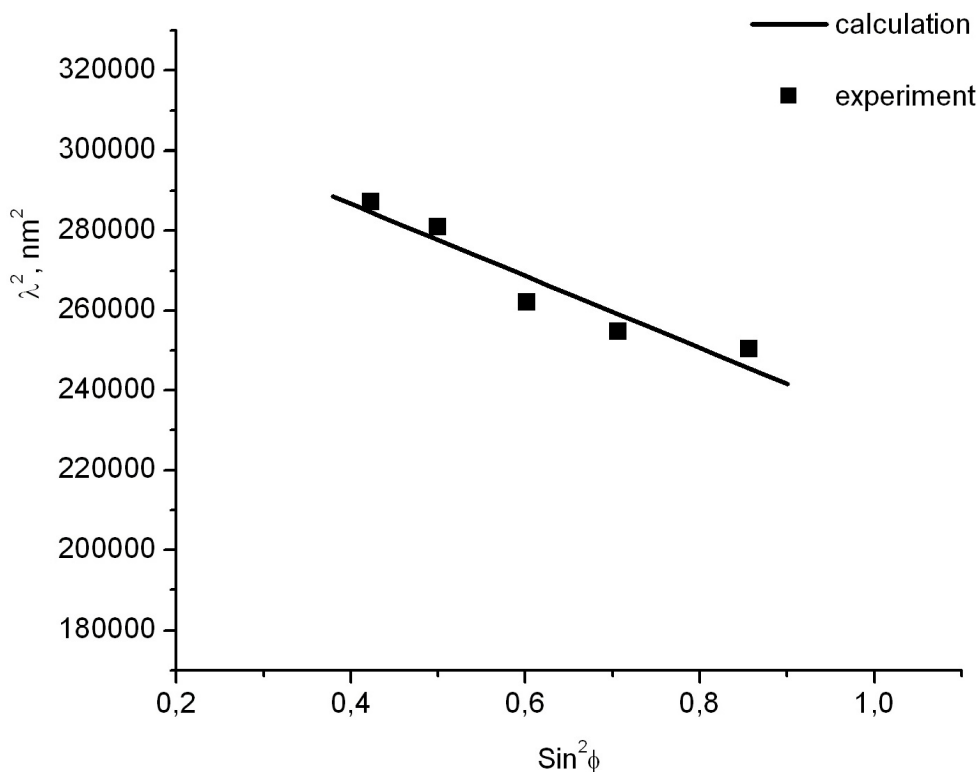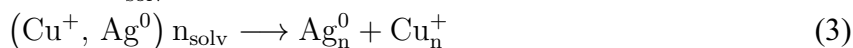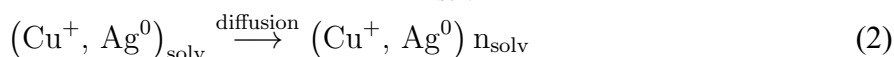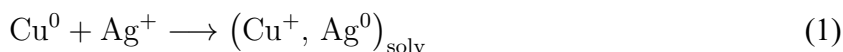
FIG. 6. Angular dispersion of the reflection peak. The dark squares are the experimental data. The solid curve is calculated using the theory of interference in thin films

Fabry–Perot interferometer (see the right part of the 5). According to common knowledge, the electrodeposition of the metal in anodic aluminum oxide occurs inside the aluminum oxide pore and is initiated near the bottom of the pore [16]. During chemical noble metal deposition, metal nanoparticles cover the open ends of the pores on the surface of the film according to the electron microscopy image (fig. 7). This is possible due to the reduction of the silver cations and oxidation of the copper nanoparticles inside the pore comes through the formation of the solvated Cu^+ intermediate cation in close contact with Ag^0 atoms. The diffusion of the solvated intermediate valence compounds (Cu^+, Ag^0) to the top of the pore leads to the formation of noble metal nanoparticles predominately on or near the surface of the AAOF. The possible reactions are shown in the scheme below.

$$Cu^0 + Ag^+ \longrightarrow \left(Cu^+, Ag^0\right)_{solv} \tag{1}$$

$$\left(Cu^+, Ag^0\right)_{solv} \xrightarrow{\text{diffusion}} \left(Cu^+, Ag^0\right) n_{solv} \tag{2}$$

$$\left(Cu^+, Ag^0\right) n_{solv} \longrightarrow Ag_n^0 + Cu_n^+ \tag{3}$$

$$Cu_n^+ + Ag_n^+ \longrightarrow Cu_n^{+2} + Ag_n^0 \tag{4}$$

$$Cu_n^+ \longrightarrow Cu_n^0 + Cu_n^{+2} \tag{5}$$

Reactions (3 – 5) occur on the surface of the film. The disproportionation of the Cu^+ intermediate cations regenerates the Cu^0 atoms (stage 5) that actively reduce silver cations on the top surface of the pore and then reactions (1 – 5) repeat with aggregation of the
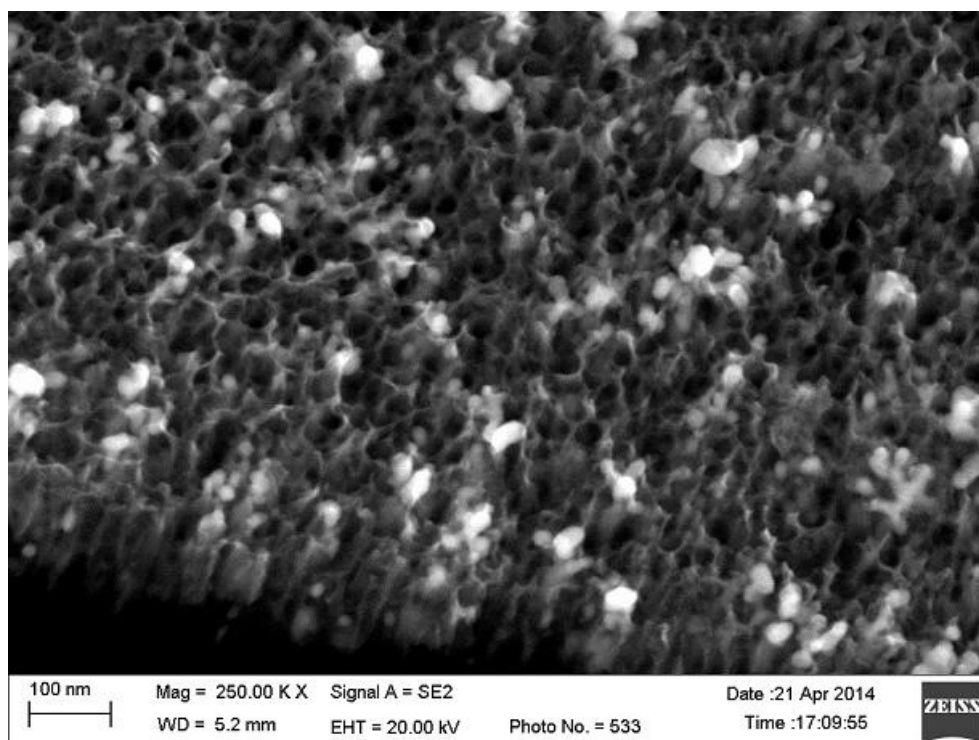
FIG. 7. The high-resolution scanning electron microscopy image of nanoporous layer of anodic aluminum oxide with sequential electrochemical (Cu) – chemical (Ag) metal deposition

silver nanoparticles on the AAOF surface. A similar reaction may occur in the case of the gold chemical deposition. By this way, the process of chemical deposition of noble metal on anodic aluminum oxide with electrochemically pre-deposited copper nanoparticles leads to the redistribution of the metal nanoparticles from the bottom and walls to the top surface of the pores. The thin surface of the Ag or Au nanoparticle-rich layer has a high contribution to the imaginary part to the complex index of the refraction due to the plasmonic nature of the nanoparticles absorption and the reflectivity of this layer became higher. Formation of the Fabrey–Perot interferometer-like nanostructure gives the effect of the mutual reflection inside the anodic aluminum oxide layer and enhances the interferometric contrast of the reflection peaks.

The porous nature of the AAOF allows it to efficiently absorb the different solvents and substances. Solvent absorption and removal reversibly changes the reflection spectra. The measured reflection spectra of the Cu–Ag metalized AAOF covered by water, ethanol and dimethylsulfoxide are shown on fig. 8. In the absence of water, the spectral maximum is located at 538 nm (see curve 1). In the presence of water, the spectral maximum is shifted to the long-wave region by 29 nm (see curve 2). A similar shift in the spectra of reflection is observed for ethanol and dimethylsulfoxide (see curve 3 and 4, respectively). The organic solvent fills porous layer and increases the refractive index of anodic aluminum oxide, so the wavelength of the reflection maximum is shifted to the long-wave spectral region. After solvent removal, the reflection maximum returns to its initial position. The observed reversible spectral shift effect gives the possibility of creating simple chemical sensors based on metalized AAOF.
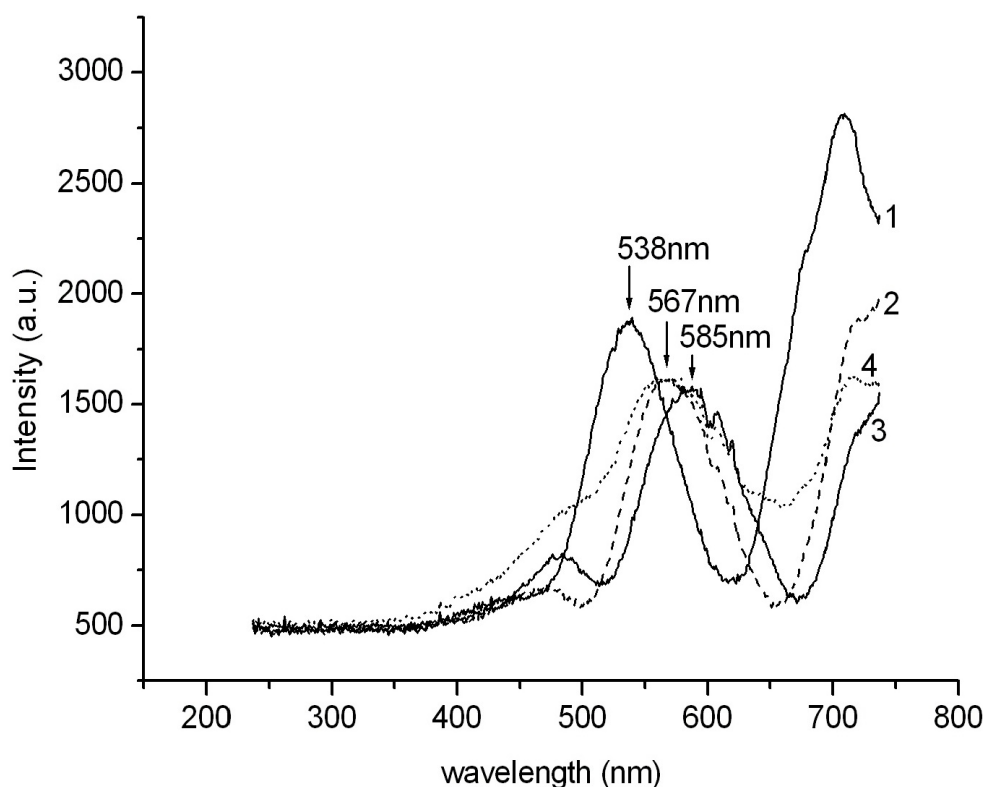
FIG. 8. Reflection spectra of Cu–Ag metalized AAOF (1) with water (2), ethanol (3) and dimethylsulfoxide (4)

4. Conclusion

The combination of the electrochemical and chemical metal deposition on the anodized aluminum film leads to the appearance of selective interference reflection colors and to the enhancement of the reflection interference contrast. Interference coloration of the anodic aluminum can be use for protective and decorative coatings. The optical reflection spectra of metalized AAOF were measured and the effective index of refraction and thickness of AAOF were calculated based on the conditions of optical wave interference. Noble metal nanoparticles were found to be redistributed to the surface of the porous layer during chemical deposition of silver and gold. The spectral shift of the reflection peaks for nanoporous metalized AAOF were shown to be dependent upon the nature of the used solvents. These phenomena are important for applications in the aerospace industry and for the manufacturing of chemical sensors.

References

[1] Moon J. M., Wei A. Uniform gold nanorod arrays from polyethylenimine-coated alumina templates. *J. Phys. Chem. B*, **109** (49), P. 23336–23341 (2005).

[2] Sauer G., Brehm G., et al. Highly ordered monociystalline silver nanowire arrays. *J. Appl. Phys.*, **91** (5), P. 3243–3247 (2002).

[3] Sauer G., Brehm G., et al. In-situ surface-enhanced Raman spectroscopy of monodisperse silver nanowire arrays. *J. Appl. Phys.*, **97**, P. 024308 (2005).

[4] Nielsch K., Muller F., Li A. P., Gosele U. Uniform nickel deposition into ordered alumina pores by pulsed electrodeposition. *Adv. Mater.*, **12** (8), P. 582–586 (2000).

[5] Belov A., Gavrilov S., Shevyakov V., Redichev E. Pulsed electrodeposition of metals into porous anodic alumina. *Applied physics A: materials science & processing*, **102**, P. 219–223 (2011).

[6] Barnakov Y. A., Kiriy N., Black P. et al. Toward curvilinear metamaterials based on silver-filled alumina templates. *Optical materials express*, **1** (6), P. 1061–1064 (2011).

[7] Ng C.K.Y. , Ngan A.H.W. Precise control of nanohoneycomb ordering over anodic aluminum oxide of square centimeter areas. *Chemistry of materials*, **23** (23), P. 5264–5268 (2011).

[8] Guo Y., Zhou L., Kameyama H. Thermal and hydrothermal stability of a metal monolithic anodic alumina support for steam reforming of methane. *Chemical engineering journal*, **168**, P. 341–345 (2011).

[9] Alam K.M., Singh A.P., Bodepudi S.C., Pramanik S. Fabrication of hexagonally ordered nanopores in anodic alumina: An alternative pretreatment. *Surface science*, **605** (3–4), P. 441–449 (2011).

[10] Atrashchenko A.V., Krasilin A.A., et al. Electrochemical methods for the synthesis of hyperbolic metamaterials. *Nanosystems: Physics, Chemistry, Mathematics*, **3** (3), P. 31–51 (2012).

[11] Chen C.Y., Huang J.H., et al. Anisotropic outputs of a nanogenerator from oblique-aligned ZnO nanowire arrays. *ACS Nano*, **5** (8), P. 6707–6713 (2011).

[12] Devan R.S., Patil R.A., Lin J.-H., Ma Y.-R. One-dimensional metal-oxide nanostructures: recent developments in synthesis, characterization, and applications. *Adv. Funct. Mater.*, **22**, P. 3326–3370 (2012).

[13] Xu D.S., Chen D.P., et al. Preparation of II-VI group semiconductor nanowire arrays by dc electrochemical deposition in porous aluminum oxide templates. *Pure and Applied Chemistry*, **72**, P. 127–135 (2000).

[14] Zhang D., Zhang H., He Y. In-situ thickness measurement of porous alumina by atomic force microscopy and the reflectance wavelength measurement from 400–1000 nm. *Microscopy Research and Technique*, **69**, P. 267–270 (2006).

[15] Masuda H., Fukuda K. Ordered metal nanohole arrays made by a two-step replication of honeycomb structures of anodic alumina. *Science*, **268** (5216), P. 1466–1468 (1995).

[16] Hwang S.K., Jeong S.H., Lee O.J., Lee K.H. Fabrication of vacuum tube arrays with a sub-micron dimension using anodic aluminum oxide nano-templates. *Microelectronic Engineering*, **77**, P. 2–7 (2005).